Photoelectron imaging of size-selected metal cluster anions in a quasi-continuous mode

Horio, Takuya
Department of Chemistry, Faculty of Science, Kyushu University

Minamikawa, Kento
Department of Chemistry, Faculty of Science, Kyushu University

Nishizato, Tasuku
Department of Chemistry, Faculty of Science, Kyushu University

Hashimoto, Haruki
Department of Chemistry, Faculty of Science, Kyushu University

他

出版情報：Review of Scientific Instruments. 93 (8), pp.083302-, 2022-08-23. AIP Publishing
バージョン：

Review of Scientific Instruments

Photoelectron imaging of size-selected metal cluster anions in a quasi-continuous mode

Cite as: Rev. Sci. Instrum. **93**, 083302 (2022); https://doi.org/10.1063/5.0097968
Submitted: 03 May 2022 • Accepted: 23 July 2022 • Published Online: 23 August 2022

Takuya Horio, Kento Minamikawa, Tasuku Nishizato, et al.

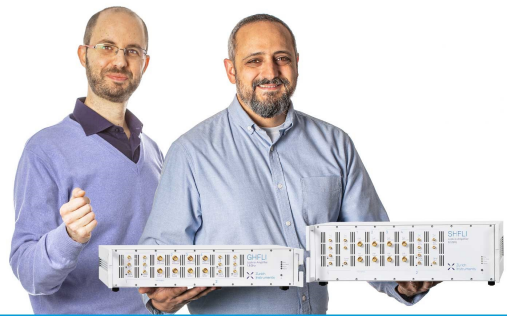

Review of Scientific Instruments ARTICLE scitation.org/journal/rsi

Photoelectron imaging of size-selected metal cluster anions in a quasi-continuous mode

Cite as: Rev. Sci. Instrum. 93, 083302 (2022); doi: 10.1063/5.0097968
Submitted: 3 May 2022 • Accepted: 23 July 2022 •
Published Online: 23 August 2022

Takuya Horio,[a] Kento Minamikawa, Tasuku Nishizato, Haruki Hashimoto, Kazuaki Matsumoto, Masashi Arakawa, and Akira Terasaki[a]

AFFILIATIONS

Department of Chemistry, Faculty of Science, Kyushu University, 744 Motooka, Nishi-ku, Fukuoka 819-0395, Japan

[a]Authors to whom correspondence should be addressed: horio@chem.kyushu-univ.jp and terasaki@chem.kyushu-univ.jp

ABSTRACT

We present a novel high-repetition-rate photoelectron imaging (PEI) apparatus for exploring electronic structures of metal cluster anions. A continuous beam of mass-selected metal cluster anions, generated by a magnetron-sputtering cluster-ion source coupled with a quadrupole mass filter, is chopped into sub-megahertz ion bunches using a high-voltage pulser. The quasi-continuous anion beam is introduced into a PEI spectrometer, where the anions are photodetached using a 404 nm (3.07 eV) continuous-wave laser diode. As a demonstration, we acquire photoelectron images for size-selected Ag cluster anions, Ag_N^- (N = 3, 7, 14), and show that each image can be obtained in a short accumulation time (50 s) with a kinetic energy resolution ($\Delta E/E$) of 4% at E = 1.77 eV. The quasi-continuous PEI technique enables high-count-rate, space-charge-free acquisition of photoelectron spectra and angular distributions not only from size-selected metal cluster anions but also from anions prepared by other continuous ion sources, such as electrospray ionization.

I. INTRODUCTION

Among various experimental techniques developed since the 1980s for exploring the size-dependent electronic structures of metal cluster anions, photoelectron spectroscopy (PES) is the gold standard. Leopold *et al.*[1] reported a pioneering PES study on metal cluster anions, in which a continuous beam of Cu cluster anions, Cu_N^- ($1 \le N \le 10$), was produced through a flowing afterglow ion source, mass-selected with a quadrupole mass filter (QMF) and photodetached with a continuous-wave (CW) Ar^+-ion laser. Using a hemispherical electron energy analyzer, they successfully measured high-resolution (<10 meV) photodetachment spectra for Cu_N^-. The combination of a CW light source and a hemispherical analyzer, referred to as "the CW mode," was originally employed in earlier anion PES studies.[2–6] Although photoelectrons are continuously generated, the acquisition of photodetachment spectra is generally time consuming because of the low electron collection efficiencies of hemispherical analyzers and because the photoelectron kinetic energy (PKE) is scanned.

Cheshnovsky *et al.*[7] presented another pioneering PES study based on a "pulsed mode," where they combined a laser vaporization cluster source (LVCS)[8–10] and a magnetic-bottle time-of-flight (MBTOF) photoelectron spectrometer.[11] Because MBTOF provides an electron collection efficiency near unity, it is indispensable for PES studies on dilute samples. In fact, it has also been implemented with other metal cluster sources, such as a pulsed arc cluster ion source (PACIS).[12] In this mode, mass selection of metal cluster anions is performed by a time-of-flight (TOF) mass spectrometer; the cluster source and mass selection are synchronized with photodetachment laser pulses. With the increasing availability of intense pulsed light sources in the visible, ultraviolet (UV), and vacuum-UV regions, numerous pulsed PES studies have been conducted not only on single-element metal clusters but also on bimetallic ones produced by dual LVCS.[13,14] Although MBTOF enables the highly efficient acquisition of photodetachment spectra, it is not suitable for obtaining angular distributions of detached photoelectrons.

Highly efficient, simultaneous measurements of photoelectron spectra and photoelectron angular distributions (PADs) can be performed by the photoelectron imaging (PEI) technique,[15] which has also been coupled with LVCS by many groups. For instance, León *et al.*[16] performed PES on vibrationally cold Au_2^- using PEI electrodes with a novel design. They further took advantage of the slow electron velocity mapping technique[17] and achieved sub-millielectron volt resolution. Melko and Castleman[18] also used PEI to explore the electronic structures of Al_N^- ($3 \le N \le 6$) clusters

produced from LVCS. Instead of LVCS or PACIS, Bartels *et al.*[19] used a gas-aggregation cluster source[20] and an ion trap to prepare cooled Na_N^- (N = 19, 40, 55, 58, 147) clusters in a pulsed manner and successfully probed the angular momentum characteristics of their valence electrons. Verlet *et al.*[21] demonstrated time-resolved PEI for metal cluster anions by investigating the electronic relaxation dynamics of Hg_N^- produced from a heated pulsed valve.

Most MBTOF-PES and PEI experiments in these pulsed modes are conducted at a repetition rate of tens of hertz because operating LVCS, PACIS, ion traps, and heated pulsed valves at high repetition rates (>1 kHz) is generally difficult. This difficulty implies that the duty cycle for the data acquisition is low ($<10^{-4}$): photoelectron TOFs are much shorter (typically 1–10 and $\ll$1 μs for MBTOF-PES and PEI, respectively) than the interval of photodetachment laser pulses (~100 ms). For such low-repetition-rate experiments, the photoelectron counts per laser shot (count rate) should be kept sufficiently low to avoid a space-charge effect, especially for slow photoelectrons. Notably, because PEI can also work for CW or quasi-CW light sources, a continuous or quasi-continuous beam of mass-selected metal cluster anions is preferable for PEI in terms of the duty cycle for data acquisition and the space-charge problem.

Here, we present a PEI apparatus operated in a "quasi-continuous mode." We generate a sub-megahertz beam of size-selected metal cluster anions using a magnetron-sputtering cluster ion source,[22] a QMF, and a potential switch (PS) originally developed for a pulsed PES for molecular anions[23] to perform PEI using a convenient CW laser diode (LD) with an emission wavelength of 404 nm (3.07 eV). In the following, we briefly outline the design considerations of the present PEI setup, describe its details, and demonstrate its performance using a Ag anion, Ag^-, and size-selected silver cluster anions, Ag_N^- (N = 3, 7, 14).

II. DESIGN CONSIDERATIONS

Most PEI spectrometers use the velocity-map imaging (VMI) configuration developed by Eppink and Parker,[24] where photoelectrons generated in a static electric field are accelerated toward a two-dimensional (2D) detector, such as a dual/triple microchannel plate (MCP) coupled with a phosphor screen. If the acceleration direction for photoelectrons is along the z-axis, two PEI spectrometer configurations are possible: an incident beam of clusters travels either parallel or perpendicular to the z-axis. In the former configuration, the 2D detector can be seriously damaged because the clusters are likely to become deposited on the detector surface. Consequently, the configuration with a beam perpendicular to the z-axis is the better choice. In our setup described in Sec. III, we use a QMF for mass selection, where the kinetic energies of the beam components in the laboratory frame after they exit the QMF are several to tens of electron volts. The beam components must therefore be accelerated such that their trajectories are not substantially deflected when they pass through the static electric field region (typically tens to hundreds of volts per centimeter) of the VMI electrodes. However, the acceleration of continuous anion beams is not straightforward because the electric potentials for each component after the QMF (e.g., einzel lens, ion deflectors, geomagnetic shielding, and VMI electrodes) must be referenced (floated) with respect to the electric potential used for anion acceleration. Although this referencing is possible, manipulating the anion beam and VMI operation is not feasible. We, therefore, developed a scheme to convert the continuous beam to a quasi-continuous one using a PS, as described in Sec. III.

III. EXPERIMENTAL SETUP

Figure 1 shows a schematic of the overall experimental setup used by our group. The major components are (a) a magnetron-sputtering cluster ion source, (b) a QMF, (c) a quadrupole ion trap, (d) a reflectron TOF mass spectrometer, and (e) a PEI spectrometer that has been developed for the present study. Components (a)–(d) have already been constructed to explore the chemical reactions between size-selected metal cluster ions and small molecules in the gas phase.[25,26] In the present study, we have used the components (a), (b), and (e). We first briefly describe components (a) and (b) and then focus on the PEI spectrometer.

A Ag target (99.99%, Kojundo Chemical Laboratory) is sputtered by Ar^+ ions, followed by clustering facilitated by a He buffer gas in a gas-aggregation cell cooled by liquid N_2. The Ag cluster anions thus produced as a continuous beam are then introduced into a He buffer gas cell also cooled by liquid N_2, where the anions are guided by an octopole ion guide (OP1) driven by a custom-made radio-frequency (rf) generator operated at a frequency of ~1 MHz. After exiting OP1, the cooled cluster anions are bent by a quadrupole deflector (QD1) and mass-selected by a QMF (MAX-4000, Extrel CMS). To optimize the Ag_N^- abundance after the mass selection, the diameter of a variable iris aperture positioned at the exit of the gas-aggregation cell and the flow rates of the Ar and He gases are adjusted; a typical direct current (DC) is 1–2 nA for Ag_3^-. The mass-selected cluster anions are further guided by octopole ion guides (OP2 and OP3) and introduced into the PEI spectrometer through QD2.

Figure 2 shows a cross-sectional view of the PEI apparatus that we built for the present study. The continuous beam of mass-selected Ag_N^- delivered through QD2 first enters a PS adjusted to +0.6 kV. The high voltage is then switched off while the accelerated anions travel inside the 25 mm-long PS, which produces anions with a 0.6 keV kinetic energy with respect to the ground potential

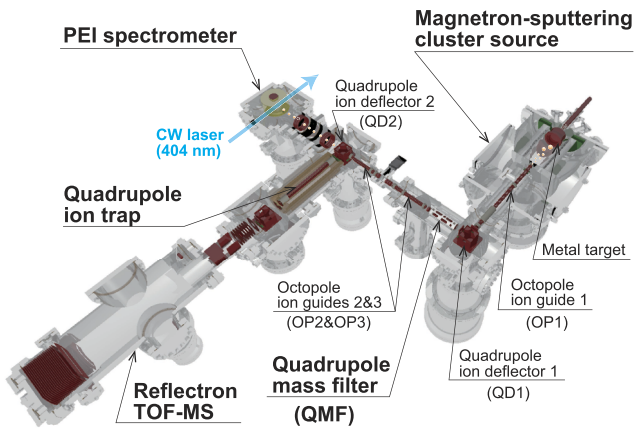

FIG. 1. Schematic of the experimental setup used in this study.

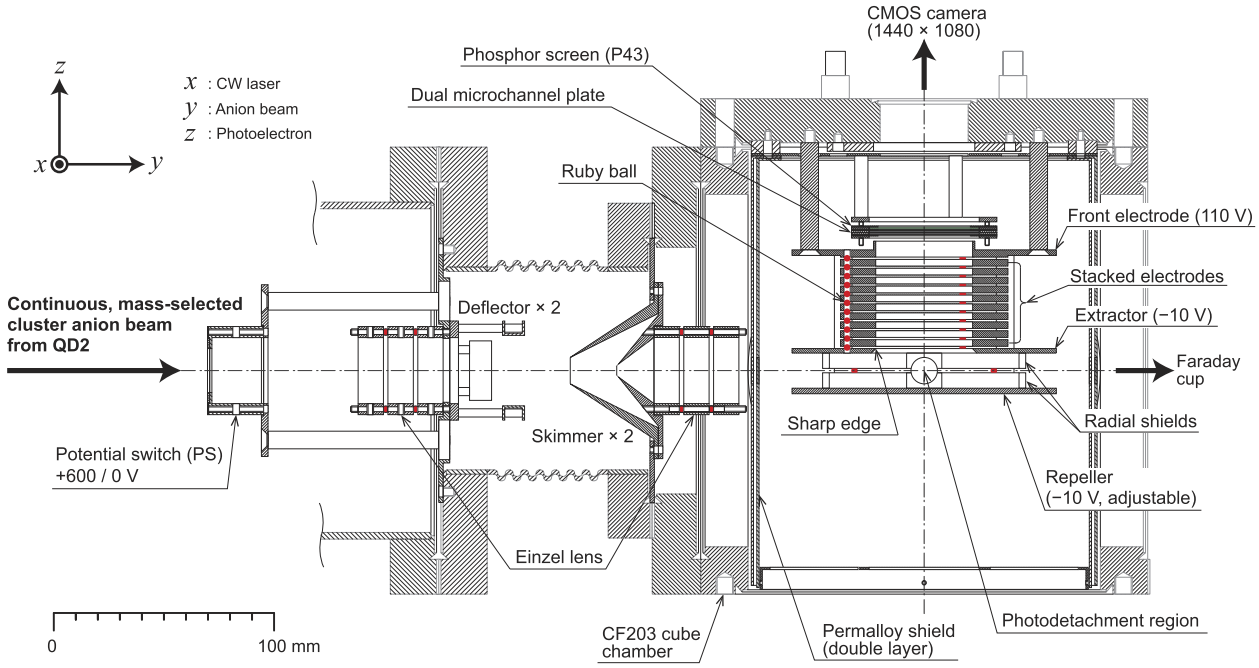

FIG. 2. Cross-sectional view of the PEI apparatus.

(0 V) when they exit the PS. On the other hand, the continuous Ag_N^- beam is interrupted while the PS potential is grounded. Consequently, the PS, driven by a high-voltage pulser (PVX-4140, DEI), transforms the continuous anion beam into a quasi-continuous one with a maximum repetition rate of 0.4 MHz.

Here, we note that because a CW light source is used for photodetachment, the duty cycle of the quasi-continuous anion beam needs to be maximized. However, its duty cycle is limited to 50% because, after the anion beam is interrupted, the operator must wait for all the accelerated anions to leave the PS before allowing subsequent anions to enter the PS by switching on the high voltage; this operation divides the anion beam into ion bunches and intervals, whose lengths are equal to those of the PS. Practically, however, at most 5% of the anions can be delivered from the PS to the photodetachment region shown in Fig. 2, as described below.

The quasi-continuous anion beam thus prepared is introduced to an assembly of VMI electrodes, which has been designed by referring to the novel PEI spectrometer developed by Horke *et al.*[27] Their design is intended to minimize the electrostatic interaction between the extraction field for photoelectrons and the incident anion beam by setting the electric field in the laser–anion interaction region as low as possible (<5 V/cm). Consequently, the deflection of the anion beam can be minimized, which enables its current to be measured with a Faraday cup (not shown in Fig. 2) while photoelectron images are recorded. Horke *et al.*[27] also pointed out a potential application of the low-extraction-field VMI electrodes to CW anion beams.

The repeller, the extractor, and the front electrode of a dual MCP backed with a P43 phosphor screen (40 mm effective diameter, PHOTONIS) are made of aluminum coated with conductive graphite. The extractor and the front electrode have an orifice (44 mm in diameter) that allows photoelectrons to pass through and create an ideal electric field for VMI. In addition, the orifice of the extractor has a sharp edge, which is inspired by the design by Wrede *et al.* for high-resolution VMI.[28] The repeller and the extractor have radial shields, which are electrically insulated with synthetic ruby balls (3 mm in diameter) so that the repeller voltage (~−10 V) can be adjusted to fine-tune the VMI condition. The repeller–extractor assembly has four 16 × 16 mm^2 square holes for the anion and photodetachment laser beams to pass through and interact with each other inside the assembly; the former and the latter propagate along the *y*- and *x*-axes, respectively (Fig. 2).

Following the original design by Horke *et al.*,[27] we first used a resistive glass tube with Ni-coated surfaces at both end faces (63.50 mm outer diameter, 48.26 mm inner diameter, and 43.9 mm length, PHOTONIS), which was sandwiched between the extractor and the front electrode, to create a constant electric field inside the glass tube and accelerate the photoelectrons toward the MCP detector. Although this design worked well, special care had to be taken to properly position the glass tube to obtain undistorted photoelectron images; even a slight displacement of the tube caused noticeable image distortion. We, therefore, replaced it with a stack of machined electrodes (Fig. 2). Ten electrodes, also made of aluminum coated with conductive graphite having an orifice (44 mm in diameter), were stacked with synthetic ruby balls (3 mm in diameter) in between for electrical insulation. These electrodes were connected by a chain of 10 MΩ resistors (not shown in Fig. 2) to create a constant electric field between the extractor (−10 V) and the front electrode (110 V); the potential of the latter is common to that

of the first (lower) plate of the MCP. The DC voltages applied to the second (upper) plate of the MCP and the phosphor screen were typically set to ~1.5 and ~4.0 kV, respectively. The VMI electrodes were suspended using polyether ether ketone (PEEK) rods, and the whole assembly was surrounded with a double-layered geomagnetic shield (permalloy).

As a photodetachment light source, a CW LD with an emission wavelength of 404 nm (3.07 eV) and a maximum output of 1000 mW (MDL-III, CNI Optoelectronics Technology) was used. The laser beam was introduced through an antireflection-coated fused silica window to the VMI electrodes, where it intersected with the quasi-continuous anion beam. The detached photoelectrons were accelerated toward the MCP, and a projected image of their three-dimensional (3D) distribution on the phosphor screen was captured using a complementary metal–oxide–semiconductor (CMOS) camera (CS165MU1/M, 1440 × 1080 pixels, Thorlabs). The 2D projection thus obtained was reconstructed to the original 3D distribution using the polar-onion-peeling (POP) algorithm[29] to obtain the photoelectron spectrum and PAD. The PKE was calibrated using the electron affinity of the Ag atom (1.302 eV).[30]

In actual measurements, we observed that the quasi-continuous Ag_N^- beam substantially diverged after leaving QD2, which made focusing all the anions onto the photodetachment region difficult. This divergence resulted in a large reduction of the anion beam intensity, for which only ~5% of the anions in the continuous beam were delivered to the VMI electrodes. Although this problem remains to be solved, photoelectron images for Ag_N^- were successfully acquired, as demonstrated in Sec. IV. Notably, because some of the anions impinged on the inner wall(s) of the repeller and/or extractor, the quasi-continuous anion beam itself created a large number of low-energy electrons, which were the background during acquisition of the laser-ON images. We, therefore, maximized the contrast of a laser-ON image to the background by carefully adjusting the pulse width and the repetition rate for the +0.6 kV pulse applied to the PS, which also functioned as an ion lens, and the DC voltages applied to the deflectors and the einzel lenses.

IV. RESULTS AND DISCUSSION

The performance of the present apparatus was tested using Ag anions, Ag^-, and their cluster anions, Ag_N^-. First, we examined the PKE resolution, which can be evaluated using a photoelectron image observed for Ag^- with the electronic configuration of $[Kr]4d^{10}5s^2$. Figures 3(a) and 4(a) show the obtained photoelectron image and the photoelectron spectra, respectively, for Ag^-, where an excess 5*s* electron is detached via a single-photon process induced by the 404 nm CW LD. The PAD characteristic of photodetachment from an *s*-orbital is clearly visualized in Fig. 3(a): a *p*-wave is expected to be a dominant partial wave because of the dipole selection rule, $\Delta l = \pm 1$, where l denotes the orbital angular-momentum quantum number.[31] The photoelectron anisotropy parameter, β, was found to be 2.00 ± 0.12, which is consistent with the aforementioned expectation as well as with the experimental value of 2 ± 0.06 reported by Sobhy and Castleman.[32] The error in our value is the standard deviation obtained by analyzing each quadrant image of Fig. 3(a). A single

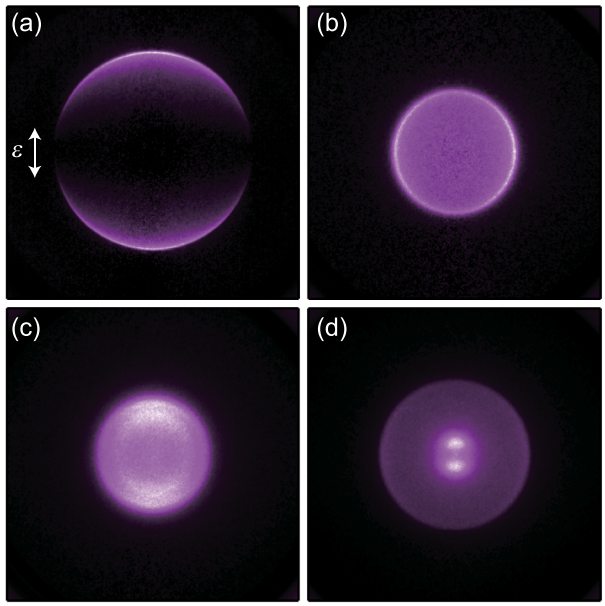

FIG. 3. Photoelectron images (2D projections) observed for (a) Ag^-, (b) Ag_3^-, (c) Ag_7^-, and (d) Ag_{14}^-. The laser-OFF background was subtracted from each image. The direction of the polarization vector, ε, is indicated by a double arrow.

peak with a full-width at half-maximum of 0.07 eV is identified in Fig. 4(a), from which the energy resolution ($\Delta E/E$) is estimated to be 4% at E = 1.77 eV. This energy resolution is similar to that reported in Ref. 27.

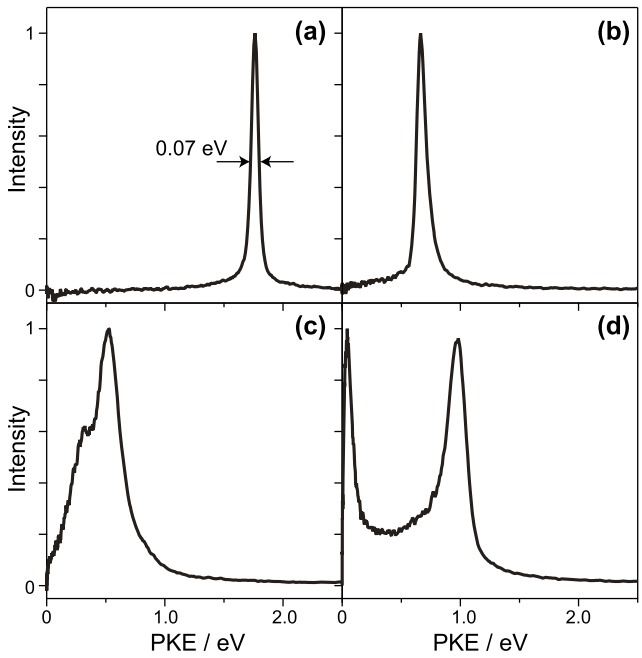

FIG. 4. Photoelectron spectra of (a) Ag^-, (b) Ag_3^-, (c) Ag_7^-, and (d) Ag_{14}^-. The intensity is in arbitrary units.

Figures 3(b)–3(d) show 2D projections of photoelectrons detached from Ag_3^-, Ag_7^-, and Ag_{14}^-, respectively. A laser-OFF background image recorded for the same accumulation time was subtracted from each image. The output of the 404 nm CW laser was 300 mW. The ion currents of the clusters were ~50, 20, and 10 pA for Ag_3^-, Ag_7^-, and Ag_{14}^-, respectively, as monitored by the Faraday cup positioned downstream of the VMI setup. The images clearly demonstrate that the present apparatus can visualize photoelectron angular anisotropies for size-selected metal cluster anions.

Figures 4(b)–4(d) present the photoelectron spectra obtained from the images in Figs. 3(b)–3(d), respectively. The vertical detachment energies (VDEs) for Ag_3^-, Ag_7^-, and Ag_{14}^- are estimated to be 2.40 ± 0.01, 2.56 ± 0.03, and 2.09 ± 0.03 eV, respectively. These values are in good agreement with those reported previously: 2.43 ± 0.01 (Ref. 30), 2.55 ± 0.1 (Ref. 30)/2.60 (Ref. 33), and 2.12 eV (Ref. 33) for Ag_3^-, Ag_7^-, and Ag_{14}^-, respectively. More details on the photoelectron spectra and PADs obtained for these cluster anions will be presented elsewhere. In the following, we discuss an advantage of our setup in terms of photoelectron signal count rates.

We highlight that the accumulation time (i.e., the total exposure time of the CMOS camera) for obtaining each image shown in Figures 3(b)–3(d) is only 50 s. This short accumulation time is due to the high repetition rate of the measurement, which is the principal advantage of the quasi-continuous operation of the present PEI spectrometer. For a quantitative discussion, we estimated the emission rate of photoelectrons, N_e, from Ag_7^-. We approximated N_e as σnlF, where σ, n, l, and F denote the photodetachment cross section of Ag_7^-, its number density, the interaction length, and the incident photon flux of the 404 nm CW laser, respectively. The number density, n, is evaluated to be ~5×10^2 cm^{-3} using the relationship $n = I_c/ev\pi(d/2)^2$, where I_c, e, v, and d are the ion current measured at the Faraday cup, the elementary charge, the translational speed of the 0.6 keV beam, and the beam diameter (~0.5 cm), respectively. The cross section, σ, is represented by the photodestruction cross section measured for Ag_7^- (~5×10^{-16} cm^2)[34] at 404 nm. We postulate l to be the diameter of the quasi-continuous anion beam.

Figure 5 shows the calculated values of N_e as a function of the power output of the 404 nm CW laser. Note that the present laser power of 300 mW yields an N_e as high as ~8×10^4 s^{-1}. Because PEI provides a collection efficiency of unity, the accumulation time of 50 s enables the collection of ~4×10^6 photoelectrons, which is sufficient to obtain a high-quality image (see Fig. 3 in Ref. 29 as an example). Furthermore, because the quasi-continuous anion beam of Ag_7^- clusters is delivered at a repetition rate of 100 kHz (10^5 s^{-1}), only "one" photoelectron is ejected at most from each ion bunch on average, as illustrated in the inset of Fig. 5. This ejection of a single electron is important in that it ensures space-charge-free measurements. The space-charge-free condition might be valid for laser powers as high as 1000 mW, where ~2.5 photoelectrons are estimated to be produced per ion bunch. The signal count rate can thus be further improved by increasing the laser power.

As for a fully CW mode, Lineberger and co-workers employed an intracavity Ar^+-ion laser with a circulating power of over 100 W, which yields ~3×10^7 s^{-1} for the calculated value of N_e assuming a collection efficiency of unity and the same values for σ, n, and l as mentioned above. However, their hemispherical analyzer only sampled 0.2% of detached electrons to achieve a high energy resolution (<1%),[35] which means that an effective value of N_e is reduced to

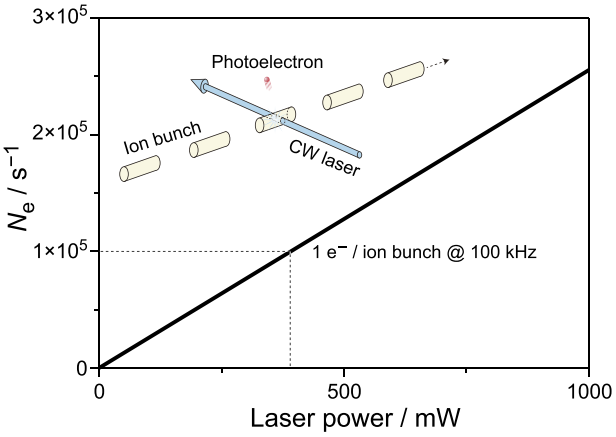

FIG. 5. The photoelectron emission rate, N_e, estimated for Ag_7^- clusters as a function of the 404 nm CW laser power. The number density and beam diameter for the clusters are ~5×10^2 cm^{-3} and ~0.5 cm, respectively. The inset schematically shows that only one photoelectron is emitted per ion bunch, ensuring space-charge-free measurements.

~6×10^4 s^{-1}. This value is comparable to that achieved in our setup with a CW light source of 0.3 W average power (~8×10^4 s^{-1}). Thus, a high-power CW laser is not necessary in the quasi-continuous PEI, if a moderate energy resolution (~4%) is acceptable.

V. SUMMARY AND PERSPECTIVE

In the present study, we developed a novel PEI apparatus dedicated to continuous anion sources. The advantage of the present technique was demonstrated for metal cluster anions generated by magnetron sputtering, where a photoelectron image was acquired within a short accumulation time under space-charge-free conditions by operating the PEI apparatus in a quasi-continuous mode. We also note that the quasi-continuous PEI method can be applied to other continuous anion sources, such as electrospray ionization.

Here, we employed a CW LD as a photodetachment light source because various convenient LDs are now commercially available at reasonable prices. Although their very small (palm-sized) footprints are advantageous in flexible layouts for constructing a PEI setup, the shortest wavelength of commercial LDs is, to the best of our knowledge, currently 375 nm (3.31 eV). CW LDs with much shorter wavelengths are strongly desired for probing electrons with higher binding energies.

An alternative is to use a quasi-CW (QCW) light source synchronized with a quasi-continuous anion beam. For instance, a regenerative amplifier (RGA) based on ytterbium-doped potassium-gadolinium tungstate (Yb:KGW) crystals is one of the available options. It delivers ~1030 nm pulses at repetition rates as high as a couple of megahertz, where the fifth harmonic (~206 nm or ~6.01 eV) is usually sufficiently high for anion photodetachment. A further advantage of Yb:KGW RGAs is that they can provide sub-picosecond ultrashort pulses, enabling time-resolved photoelectron imaging (TRPEI) with the present setup, where photoelectron images will be obtained with an unprecedented signal-to-noise ratio in a short accumulation time. Negative-to-neutral-to-positive ion

(NeNePo) pump–probe spectroscopy developed by Wolf *et al.*[36] inspires us to visualize nuclear dynamics of clusters by TRPEI. For example, photodetachment from linear-shaped Ag_3^- by a pump pulse creates a vibrational wave packet on the ground electronic state of neutral Ag_3, which propagates on the potential-energy surface toward its triangular equilibrium geometry. Nuclear motion can be observed in time-resolved photoelectron images acquired by photoionization with a time-delayed probe pulse. Such an experiment is in progress in our group.

ACKNOWLEDGMENTS

This work was supported by Grants-in-Aid for Challenging Research (Exploratory) (Grant No. JP20K21177) and Scientific Research (A) (Grant No. JP18H03901) from the Japan Society for Promotion of Science (JSPS), the Research Foundation for Opto-Science and Technology, the Murata Science Foundation, and the Grant for Basic Science Research Projects from the Sumitomo Foundation (Grant No. 200378). T.H. gratefully acknowledges Professor Jan R. R. Verlet for fruitful discussion on the design of the PEI spectrometer and for providing us with the POP algorithm.

AUTHOR DECLARATIONS

Conflict of Interest

The authors have no conflicts to disclose.

Author Contributions

Takuya Horio: Conceptualization (lead); Formal analysis (equal); Funding acquisition (equal); Investigation (equal); Methodology (lead); Writing – original draft (lead); Writing – review & editing (equal). **Kento Minamikawa**: Formal analysis (equal); Investigation (equal); Methodology (supporting). **Tasuku Nishizato**: Formal analysis (equal); Investigation (equal); Methodology (supporting). **Haruki Hashimoto**: Investigation (supporting). **Kazuaki Matsumoto**: Investigation (supporting). **Masashi Arakawa**: Funding acquisition (equal); Supervision (supporting); Writing – review and editing (equal). **Akira Terasaki**: Funding acquisition (equal); Project administration (lead); Supervision (lead); Writing – review and editing (equal).

DATA AVAILABILITY

The data that support the findings of this study are available from the corresponding authors upon reasonable request.

REFERENCES

[1] D. G. Leopold, J. Ho, and W. C. Lineberger, J. Chem. Phys. **86**, 1715 (1987).
[2] B. Brehm, M. A. Gusinow, and J. L. Hall, Phys. Rev. Lett. **19**, 737 (1967).
[3] M. W. Siegel, R. J. Celotta, J. L. Hall, J. Levine, and R. A. Bennett, Phys. Rev. A **6**, 607 (1972).
[4] A. Kasdan, E. Herbst, and W. C. Lineberger, J. Chem. Phys. **62**, 541 (1975).
[5] H. B. Ellis and G. B. Ellison, J. Chem. Phys. **78**, 6540 (1983).
[6] J. V. Coe, J. T. Snodgrass, C. B. Freidhoff, K. M. McHugh, and K. H. Bowen, J. Chem. Phys. **84**, 618 (1986).
[7] O. Cheshnovsky, S. H. Yang, C. L. Pettiette, M. J. Craycraft, and R. E. Smalley, Rev. Sci. Instrum. **58**, 2131 (1987).
[8] T. G. Dietz, M. A. Duncan, D. E. Powers, and R. E. Smalley, J. Chem. Phys. **74**, 6511 (1981).
[9] V. E. Bondybey and J. H. English, J. Chem. Phys. **74**, 6978 (1981).
[10] M. A. Duncan, Rev. Sci. Instrum. **83**, 041101 (2012).
[11] P. Kruit and F. H. Read, J. Phys. E: Sci. Instrum. **16**, 313 (1983).
[12] C. Y. Cha, G. Ganteför, and W. Eberhardt, Rev. Sci. Instrum. **63**, 5661 (1992).
[13] S. Nonose, Y. Sone, K. Onodera, S. Sudo, and K. Kaya, J. Phys. Chem. **94**, 2744 (1990).
[14] A. Nakajima, K. Hoshino, T. Naganuma, Y. Sone, and K. Kaya, J. Chem. Phys. **95**, 7061 (1991).
[15] H. Helm, N. Bjerre, M. J. Dyer, D. L. Huestis, and M. Saeed, Phys. Rev. Lett. **70**, 3221 (1993).
[16] I. León, Z. Yang, H.-T. Liu, and L.-S. Wang, Rev. Sci. Instrum. **85**, 083106 (2014).
[17] A. Osterwalder, M. J. Nee, J. Zhou, and D. M. Neumark, J. Chem. Phys. **121**, 6317 (2004).
[18] J. J. Melko and A. W. Castleman, Jr., Phys. Chem. Chem. Phys. **15**, 3173 (2013).
[19] C. Bartels, C. Hock, J. Huwer, R. Kuhnen, J. Schwöbel, and B. von Issendorff, Science **323**, 1323 (2009).
[20] I. M. Goldby, B. von Issendorff, L. Kuipers, and R. E. Palmer, Rev. Sci. Instrum. **68**, 3327 (1997).
[21] J. R. R. Verlet, A. E. Bragg, A. Kammrath, O. Cheshnovsky, and D. M. Neumark, J. Chem. Phys. **121**, 10015 (2004).
[22] H. Haberland, M. Karrais, M. Mall, and Y. Thurner, J. Vac. Sci. Technol. A **10**, 3266 (1992).
[23] L. A. Posey, M. J. Deluca, and M. A. Johnson, Chem. Phys. Lett. **131**, 170 (1986).
[24] A. T. J. B. Eppink and D. H. Parker, Rev. Sci. Instrum. **68**, 3477 (1997).
[25] S. Sarugaku, M. Arakawa, T. Kawano, and A. Terasaki, J. Phys. Chem. C **123**, 25890 (2019).
[26] T. Handa, T. Horio, M. Arakawa, and A. Terasaki, Int. J. Mass. Spectrom. **451**, 116311 (2020).
[27] D. A. Horke, G. M. Roberts, J. Lecointre, and J. R. R. Verlet, Rev. Sci. Instrum. **83**, 063101 (2012).
[28] E. Wrede, S. Laubach, S. Schulenburg, A. Brown, E. R. Wouters, A. J. Orr-Ewing, and M. N. R. Ashfold, J. Chem. Phys. **114**, 2629 (2001).
[29] G. M. Roberts, J. L. Nixon, J. Lecointre, E. Wrede, and J. R. R. Verlet, Rev. Sci. Instrum. **80**, 053104 (2009).
[30] J. Ho, K. M. Ervin, and W. C. Lineberger, J. Chem. Phys. **93**, 6987 (1990).
[31] J. Cooper and R. N. Zare, J. Chem. Phys. **48**, 942 (1968).
[32] M. A. Sobhy and A. W. Castleman, J. Chem. Phys. **126**, 154314 (2007).
[33] H. Handschuh, C. Y. Cha, P. S. Bechthold, G. Ganteför, and W. Eberhardt, J. Chem. Phys. **102**, 6406 (1995).
[34] J. Tiggesbäumker, L. Köller, and K.-H. Meiwes-Broer, Chem. Phys. Lett. **260**, 428 (1996).
[35] D. G. Leopold, K. K. Murray, A. E. S. Miller, and W. C. Lineberger, J. Chem. Phys. **83**, 4849 (1985).
[36] S. Wolf, G. Sommerer, S. Rutz, E. Schreiber, T. Leisner, L. Wöste, and R. S. Berry, Phys. Rev. Lett. **74**, 4177 (1995).